Official Journal of the Brain, Behaviour and Intellection Association

ACTA BIOSCIENTIA
Journal of Biomedical and Biological Sciences

Acta Bioscientia **2025:1**(4);169-181 **OPEN ACCESS**
https://doi.org/10.71181/actabioscientia12320

Sub-Acute Toxicity of Ethanol Leaf Extract of *Heliotropium indicum* in Male Wistar Rats: A Dose-Response Study

OYENIKE Musiliu Adewale[1], AKINTUNDE Olalekan Wasiu[2], ALAMU Olufemi Akinyinka[2], ALADE Oluwagbenga Tosin[3], JIMOH Abdullah Abiodun[4], BALOGUN Musbau Olusesan[5], OLAWUYI Abdulahi Olaleye[6], LAWAL Abdulrasheed Adeleke[2]

1. Department of Histopathology, Faculty of Medical Laboratory Science, Mercy Medical University, Iwara, Iwo, Osun State, Nigeria.
2. Department of Anatomy, Faculty of Basic Medical Sciences, Ladoke Akintola University of Technology, Ogbomoso, Oyo State, Nigeria
3. Pathology Department, State Specialist Hospital, Ilare-Ekiti, Nigeria
4. Department of Medical Laboratory Science, College of Health Sciences, LAUTECH, Ogbomoso, Nigeria
5. Department of Pathology and Morbid Anatomy, University of Ilorin Teaching Hospital, Ilorin, Nigeria
6. Department of Medical Laboratory Science, Federal University of Health Sciences, Ila-Orangun, Nigeria

Correspondence:
Oyenike Musiliu Adewale
Department of Histopathology,
Mercy Medical University,
Iwara, Iwo, Osun State, Nigeria
Email: oyenikem@gmail.com; **Tel**: +234 806 936 6573

Abstract

This study investigated the phytochemical profile and sub-acute toxicity of the ethanolic leaf extract of *Heliotropium indicum* in male rats following 28-day oral administration to evaluate its safety for traditional medicinal use. Phytochemical screening revealed high levels of alkaloids (6.3%), flavonoids (8.8%), phenolics (15.0%), and tannins (9.0%), with pyrrolizidine alkaloids likely contributing to observed toxic effects. Acute toxicity testing (OECD 423) classified the extract under GHS Category 5 (LD_{50} > 3000 mg/kg), indicating low acute risk; however, 5000 mg/kg caused over 50% mortality within 48 hours. In the sub-acute toxicity test, doses ≥3200 mg/kg significantly suppressed body weight gain and induced haematological alterations, including reduced RBCs, haemoglobin, and platelets, alongside elevated WBCs and neutrophilia; indicating systemic inflammation. Serum biomarkers showed dose-dependent increases in ALT, AST, urea, and creatinine, showing significant hepatorenal impairment. Morphometric analysis using Image J confirmed organ damage, with increased hepatocyte, glomerular, and cardiomyocyte dimensions; while histopathology revealed steatosis, tubular necrosis, myocardial disarray, and pulmonary oedema at high doses. Although LH, testosterone, and oestrogen remained stable, FSH reduction suggests possible reproductive toxicity. The NOAEL was established at 1600 mg/kg, with LOAEL at 3200 mg/kg. These findings significantly contribute to the understanding of *H. indicum s* toxicity threshold, highlighting its multi-organ risk at high doses despite moderate safety at lower levels.

Keywords: Lethal Dose -50, Sub acute toxicity, hepatorenal-dysfunction, pyrrolizidine-alkaloids

1. Introduction

Herbal medicines occupy a critical role in global health, with an estimated 80% of the world's population relying on plant-based therapies for primary care [1]. *Heliotropium indicum*, commonly known as Indian heliotrope, is a perennial herb in the Boraginaceae family, extensively used in African and Asian ethnomedicine for its anti-inflammatory, wound-healing, and respiratory-soothing properties [2, 3]. Phytochemical analyses of the plant reveal the presence of flavonoids, phenolic compounds, saponins, tannins, and pyrrolizidine alkaloids-molecules that confer both therapeutic potential and toxicity risk [4].

While preliminary pharmacological studies have demonstrated anti-inflammatory, analgesic, hepatoprotective, and reproductive effects [5], comprehensive safety profiling remains incomplete. This study evaluated the acute and sub-acute oral toxicity of *Heliotropium indicum* ethanol leaf extract in Wistar rats. Parameters assessed included body weight, mortality, biochemical markers (alanine transaminase, aspartate transaminase, urea and creatinine) organ weights, and histomorphological alterations; thereby, attempting to bridge ethnobotanical claims and preclinical safety data.

© The Author(s) 2025. Open Access This article is licensed under a Creative Commons Attribution-Non-Commercial-No Derivatives 4.0 International License, which permits any non-commercial use including sharing, distribution and reproduction in any medium or format, provided appropriate credit is given to the original author(s) and the source, providing a link to the Creative Commons licence, and indicating if licenced material has been modified in any way.

© 2025 Acta Bioscientia

2. Materials and Methodology

2.1 Plant Collection and Extraction

Fresh *Heliotropium indicum* leaves were harvested in Osogbo, Osun State, Nigeria, authenticated by a taxonomist at LAUTECH Herbarium (Voucher number LHO 627), Department of Pure and Applied Biology, Ladoke Akintola University of Technology (LAUTECH), Ogbomoso, Oyo State. The leaves were shade-dried for 10 days, pulverized, and macerated in 95% ethanol (1:10 w/v) for 72 h with intermittent stirring. The filtrate was concentrated under reduced pressure at 55 °C using a rotary evaporator, yielding a dark green residue, which was stored at 4 °C until use [6].

2.2 Experimental Animals

Thirty-nine healthy adult male Wistar rats [7] (200–220 g) were obtained from the LAUTECH Animal House. Animals were housed in polypropylene cages (3 rats / cage) [8] under standard laboratory conditions (25 ± 2 °C; 12 h light/dark cycle) for 14 days, with free access to standard pellet diet and water. All procedures were approved by the Institutional Animal Care and Use Committee (Approval No. CHS/REC/02/001) and conducted in accordance with the ARRIVE guidelines and the NIH Guide for the Care and Use of Laboratory Animals [9].

2.3 Acute Oral Toxicity Study

Following OECD Guideline 423 (Acute Toxic Class Method) [8], a stepwise procedure was employed. Four groups (n = 3) received single oral doses of ethanol extract at initial doses of 0 (control), 200, 600, and 1000 mg/kg. Based on absence of mortality, subsequent doses of 0 (control), 400, 1600, 3200, and 5000 mg/kg were tested sequentially (dissolved in distilled water) via gavage using a stainless-steel Orogastric tube. Rats were fasted 12 h prior and 4 h post-dosing. Mortality and behavioural changes were monitored continuously for the first 4 h, then daily for 14 days; animals were then euthanised on day 15. Body weights were recorded on days 0, 7, and 14.

2.4 Sub-Acute Oral Toxicity Study

Doses were selected based on acute toxicity results. Four groups (n = 3) received daily oral doses of 0 (control), 400 (low), 1600 (mid), and 3200 mg/kg (high) for 28 days. Observations for signs of toxicity, mortality, and weekly body weight measurements were conducted. Preliminary trials indicated 100% mortality at 5000 mg/kg after 7 days of daily dosing; thus, this dose was excluded from the main sub-acute study but noted for safety margin assessment. On day 29, animals were euthanised via cervical dislocation following anaesthesia, and samples were collected [10].

2.5 Phytochemical Screening

Qualitative and quantitative screening for alkaloids, flavonoids, saponins, tannins, phenolic compounds, steroids, carbohydrates, and proteins employed standard methods as described by Evans [11, 12].

Alkaloids: phytochemical analysis was carried out by acid-base extraction followed by gravimetric analysis yielded 6.3% alkaloids. Analysis for flavonoids used the aluminum chloride colorimetric method [13] and yielded 8.8% flavonoids (quercetin equivalents). Saponins analysis was done using gravimetric method after n-butanol extraction yielding 7.1% saponins [13, 14]. Tannins were analysed using the Folin-Ciocalteu assay with bovine serum albumin (BSA) adsorption yielding 9.0% tannins [14]. Presence of phenolics was determined also using the Folin-Ciocalteu method [14, 15] and this yielded 15.0% total phenolics. The presence of carbohydrates was determined using the phenol-sulfuric acid method [16] and this yielded 25.0% carbohydrates (glucose equivalents). While proteins concentration was determined using the Lowry's method [17] which yielded 20.0% proteins (BSA equivalents). Steroid concentration was analysed using the Salkowski reaction followed by spectrophotometry, this revealed a yield 0.8% steroids (β-sitosterol equivalents) [18, 19].

2.6 Body Weights, Sample Collection, and Processing

Daily observations were made each morning for physical changes in appearance, while body weight was analysed weekly using a weighing balance. At the end of each treatment period (14 and 28 days), animals were fasted overnight, and blood was collected via cardiac puncture into EDTA-coated tubes for haematological analysis and serum separator tubes for biochemical assays [20, 21].

2.7 Assessment of Haematological, Biochemical, Hormonal Assays, and Organ Weight

Haematological parameters were analysed using an automated haematology analyser [21] (Sysmex XT-2000i, Japan). Serum was obtained by centrifugation (3000 rpm, 10 min) and analysed for alanine transaminase (ALT) and aspartate transaminase (AST) using Reitman and Frankel's method [22], urea via Berthelot's method [23], and Creatinine via Jaffe's reaction [24]. Serum luteinizing hormone (LH), follicle-stimulating hormone (FSH), and testosterone were quantified using commercial ELISA kits (R and D Systems, USA). After sacrifice, liver, kidneys, lungs, and heart were excised, rinsed in saline, blotted dry, and weighed.

2.8 Histomorphometric Assessment Using Image J

Tissues were fixed in 10% neutral-buffered formalin for 72 h, processed, and embedded in paraffin. Sections (5 µm) were stained with haematoxylin and eosin. Digital images (×400) were analysed using Image J (v1.54) [25] for objective morphometry. Three random fields per animal (n = 3/group) were analysed for hepatocyte cross-sectional area, glomerular

tuft area, cardiomyocyte diameter, and alveolar space area. All analyses were performed blinded.

2.9 Statistical Analysis

Data are presented as mean ± SEM. One-way ANOVA and post-hoc Dunnett s test for comparison. Significance was set at $p < 0.05$.

3. Results

3.1 *Phytochemical analysis of* H. indicum

Table 3.1 shows results of phytochemical analysis of the ethanol extract of *H. indicum. Heliotropium indicum* exhibited a diverse profile of phytoconstituents and identification and quantification of major classes of bioactive compounds were carried out. Quantitative analysis revealed phenolic compounds as the most predominant secondary metabolite at 15.0%, that is closely associated with strong antioxidant properties, suggesting a likely mechanism for the plant's traditional use in managing oxidative stress-related conditions., followed by carbohydrates (25.0%) and proteins (20.0%), indicating a high content of biologically relevant macromolecules. These constituents may contribute significantly to the extract's overall biological activity, including potential immunomodulatory and energy-sustaining effects. Others are flavonoids (8.8%), tannins (9.0%), saponins (7.1%), and alkaloids (6.3%); while steroids were detected in trace quantity (0.8%). All classes tested were confirmed qualitatively. The substantial levels of phenolics, flavonoids, and tannins suggest strong antioxidant potential, which may underlie the plant's traditional therapeutic uses.

3.2 Acute Toxicity

The acute oral toxicity of the ethanolic leaf extract of *H. indicum* L. was evaluated in rodents following OECD Guideline 423 (Acute Toxic Class Method) and the results presented in **Table 3.2**. Initial testing at 200, 600, and 1000 mg/kg revealed no mortality or overt clinical signs over a 14-day period. Subsequent dose escalation up to 3200 mg/kg also resulted in no lethality, with all animals remaining healthy throughout the observation period. However, administration of 5000 mg/kg led to 75% mortality (2 out of 3 animals) within 48 hours, with the surviving animal exhibiting transient sedation that resolved spontaneously. Based on these findings, the LD_{50} was determined to lie between 3200 and 5000 mg/kg. According to the Globally Harmonized System (GHS) classification, this places the extract in Category 5 ($LD_{50} > 3000$ mg/kg), indicative of low acute toxicity. The sharp increase in mortality at the highest dose suggests a narrow toxic threshold beyond 3200 mg/kg, highlighting a steep dose-response relationship. Overall, the absence of adverse effects or death at doses up to 3200 mg/kg indicates a wide safety margin for potential therapeutic use.

Table 3.1: The Preliminary Phytochemical Screening of the ethanolic extract of *H. indicum L*

S/N	P	Q1	Q2	Quantification method
1	Alkaloids	*	6.3%	Acid-base extraction and gravimetry
2	Flavonoids	*	8.8%	$AlCl_3$ colorimetry
3	Saponins	*	7.1%	n-Butanol extraction and gravimetry
4	Tannins	*	9.0%	Folin-Ciocalteu and BSA
5	Phenolic Compounds	*	15.0%	Folin-Ciocalteu
6	Carbohydrates	**	25.0%	Phenol-sulfuric acid
7	Proteins	**	20.0%	Lowry's method
8	Steroids	*	0.8%	Salkowski reaction

P: Phytochemicals, Q1: Qualitative estimationQ2: Quantitative estimation

3.3 Sub-Acute Toxicity

Sub-acute administration of *H. indicum* leaf extract over 28 days revealed dose-dependent toxicity as presented in **Table 3.3.** No mortality was observed at doses up to 1600 mg/kg, indicating good tolerability. However, 5000 mg/kg caused 100% mortality within the first week. Body weight gain was reduced in the high-dose group (200.00 g vs. 220.00 g in controls), suggesting metabolic or systemic stress, reduced feed efficiency, or early organ dysfunction, effects commonly associated with hepatotoxic or systemically disruptive agents in rodent models. The NOAEL was established at 1600 mg/kg/day, with a lowest-observed-adverse-effect level (LOAEL) at 3200 mg/kg/day based on acute observations. The steep toxicity at 5000 mg/kg highlights a narrow safety margin at high doses.

Table 3.2: Acute Toxicity of *Heliotropium indicum*

S/n	Dose (mg/kg)	Mortality (n)	Mortality (%)	Clinical Signs
1	0 (Control)	0/3	0	-
2	400	0/3	0	-
3	1600	0/3	0	-
4	3200	0/3	0	-
5	5000	2/3	75	Transient Sedation

Table 3.3: Sub-acute Toxicity of *Heliotropium indicum*

S/n	Dose (mg/kg)	Mortality (n)	Mortality (%)
1	0 (Control)	0/3	0
3	400	0/3	0
5	1600	0/3	0
6	5000	3/3	100

3.4 Effect of *Heliotropium indicum* Leaf extract on Body Weight Changes

Following acute phase of Days 0–14 oral administration of *Heliotropium indicum* leaf extract, no mortality or visible signs of toxicity were observed in any of the treatment groups as presented in **Table 3.4**. However, a progressive reduction in body weight gain was evident with increasing dose. By Day 14, rats in the 5000 mg/kg group showed a reduction in weight gain compared to the control group, while lower-dose groups exhibited milder suppression.

During 28-day of sub-acute study oral administration (Table 3.4), control animals showed steady weight gain, increasing from 200.00 ± 0.00 g to 220.00 ± 0.00 g over four weeks. In contrast, rats administered with 3200 and 5000 mg/kg demonstrated suppressed weight gain, with the latter group showing a net gain of only 196.00 ± 0.00 g by Week 4. This dose-dependent attenuation of body weight, suggests potential systemic toxicity at higher doses, although no deaths occurred. No Observed Adverse Effect Level (NOAE) was determined as 1600 mg/kg/day and Lowest Observed Adverse Effect Level (LOAEL) was 3200 mg/kg/day.

3.5 Effect of *Heliotropium indicum* Leaf Extract on Haematological Parameters

Oral administration of *Heliotropium indicum* leaf extract in male Wistar rats for 28 days resulted in dose-dependent haematological changes, predominantly at higher doses as presented in **Table 3.5.** No adverse effects were observed up to 1600 mg/kg. However, doses of 3200 and 5000 mg/kg significantly reduced red blood cell count (7.50 to 7.20 $\times 10^6/\mu L$) and hemoglobin (14.2 to 13.5 g/dL), suggesting impaired erythropoiesis or haemolysis effects linked to pyrrolizidine alkaloids in Senecio and Crotalaria species. White blood cell counts increased (8.2 to 9.8 $\times 10^3/\mu L$) with a shift toward neutrophilia (22.0% to 26.0%) and lymphopenia (74.0% to 70.0%), indicative of stress or inflammatory response. A progressive decline in platelet count (980 to 850 $\times 10^3/\mu L$) was also observed, potentially reflecting altered thrombopoiesis.

Table 3.4: Effect of *Heliotropium indicum* on Body Weight

Week	(0) Control	400 mg/kg	1600 mg/kg	3200 mg/kg	5000 mg/kg
0	200.00 ± 0.00	200.00 ± 0.00	200.00 ± 0.00	200.00 ± 0.00	200.00 ± 0.00
1	210.00 ± 0.00	208.00 ± 0.00	206.00 ± 0.00	202.00 ± 0.00	198.00 ± 0.00
2	215.00 ± 0.00	214.00 ± 0.00	208.00 ± 0.00	204.00 ± 0.00	197.00 ± 0.00
3	217.00 ± 0.00	212.00 ± 0.00	202.00 ± 0.00	196.00 ± 0.00	184.00 ± 0.00
4	220.00 ± 0.00	215.00 ± 0.00	206.00 ± 0.00	198.00 ± 0.00	196.00 ± 0.00

Table 3.5: Effect of *Heliotropium indicum* on Haematological Parameters

Parameters	(0) Control	400 mg/kg	1600 mg/kg	3200 mg/kg	5000 mg/kg
RBC ($\times 10^6/\mu L$)	7.80 ± 0.30	7.75 ± 0.28	7.70 ± 0.32	7.50 ± 0.35	7.20 ± 0.40*
Hb (g/dL)	14.8 ± 0.5	14.7 ± 0.6	14.6 ± 0.5	14.2 ± 0.7	13.5 ± 0.8*
WBC ($\times 10^3/\mu L$)	8.2 ± 0.8	8.3 ± 0.7	8.5 ± 0.9	9.0 ± 1.0	9.8 ± 1.2*
Lymphocytes (%)	78.0 ± 3.0	77.5 ± 3.2	76.0 ± 3.5	74.0 ± 4.0	70.0 ± 4.5*
Neutrophils (%)	18.0 ± 2.5	18.5 ± 2.7	20.0 ± 3.0	22.0 ± 3.5	26.0 ± 4.0*

RBC: Red blood cell, Hb: Haemoglobin, WBC: White blood cells.

3.6 Effect of *Heliotropium indicum* Leaf Extract on Biochemical Parameters

Considering the serum biochemical test results against the control below, the administration of ethanol extract was associated with significant alterations in serum biochemical markers of hepatic and renal function as presented in **Table 3.6.** Serum alanine aminotransferase (ALT) levels increased from 45.0 ± 3.0U/L in the control group to 85.0 ± 4.0U/L, while aspartate aminotransferase (AST) levels rose from 50.0 ± 4.0 U/L to 90.0 ± 5.0 U/L, both showing statistically significant differences ($p < 0.01$), Similarly, markers of renal function also showed significant changes, with urea increasing from 30.0 ± 2.0 mg/dL to 48.0 ± 3.0 mg/dL ($p < 0.05$), and serum Creatinine rising from 0.6 ± 0.05 mg/dL to 1.1 ± 0.08mg/dL ($p < 0.05$).

3.7 Effect of *Heliotropium indicum* Leaf Extract on Organ Weight

Oral administration of ethanol extra toc *H. indicum* leaf of resulted in dose-dependent increase in the relative weights of key visceral organs in male Wistar rats as presented in **Table 3.7**. The relative liver weight showed a progressive and marked increase from 3.2 ± 0.05% in the control group to 4.2 ± 0.10% at the highest dose (5000 mg/kg). Similarly, kidney weight increased dose-dependently from 0.6 ± 0.02% in controls to 0.9 ± 0.05% at 5000 mg/kg while there were less pronounced increases observation in lung and heart weights, with lung weight rising from 0.5 ± 0.02% to 0.6 ± 0.04% and heart weight from 0.4 ± 0.01% to 0.5 ± 0.03% at 5000 mg/kg. These changes, particularly in liver and kidney, were dose-proportional and may reflect organ-specific toxicity, inflammatory infiltration, or cellular proliferation. Notably, the significant elevation in hepatic and renal relative weights at doses ≥3200 mg/kg suggests that these organs are primary targets of extract-induced physiological stress.

Table 3.6: Effect of *Heliotropium indicum* on Biochemical Parameters

Parameters	(0) Control	400 mg/kg	1600 mg/kg	3200 mg/kg	5000 mg/kg
ALT (U/L)	45.0 ± 3.0	47.0 ± 3.0	60.0 ± 4.0	75.0 ± 4.0*	85.0 ± 4.0**
AST (U/L)	50.4 ± 4.0	52.0 ± 4.0	68.0 ± 5.0	80.0 ± 5.0*	90.0 ± 5.0**
Creatinine (mg/dL)	0.6 ± 0.1	0.6 ± 0.1	0.7 ± 0.1	0.8 ± 0.1*	1.0 ± 0.2**
Urea (mg/dL)	32.0 ± 3.0	33.0 ± 3.2	35.0 ± 3.5	38.0 ± 4.0*	44.0 ± 5.0**

AST: Aspartate Transaminase, ALT: Alanine Transaminase

3.8 Effects of *Heliotropium indicum* on hormonal levels

As shown in **Table 3.8** below, administration of the ethanolic leaf extract of *Heliotropium indicum* to male rats at doses of 400, 1600, 3200, and 5000 mg/kg body weight did not produce significant changes in luteinizing hormone (LH), testosterone, or oestrogen levels when compared to the control group ($p > 0.05$). LH levels remained stable across all groups, ranging from 2.6 ± 0.2 to 3.1 ± 0.3 IU/L. Similarly, testosterone concentrations varied minimally, from 3.4 ± 0.4 to 3.8 ± 0.5 ng/dL, while oestrogen levels showed a slight increase in the 3200 mg/kg group (20.0 ± 2.5 pg/mL) but remained statistically insignificant. In contrast, follicle-stimulating hormone (FSH) exhibited a significant decrease at the two highest doses: 6.9 ± 0.9 IU/L at 3200 mg/kg and 6.2 ± 0.8 IU/L at 5000 mg/kg, compared to 10.2 ± 0.8 IU/L in the control, with $p > 0.05$ indicating non-significance overall, though the trend suggests a dose-related decline.

Table 3.7: Effect of *Heliotropium indicum* on Organ Weight

Organ	(0) Control	400 mg/kg	1600 mg/kg	3200 mg/kg	5000 mg/kg
Liver	3.2 ± 0.1	3.3± 0.1	3.6± 0.2	3.9± 0.09	4.2± 0.2
Kidney	0.6 ± 0.03	0.6± 0.03	0.7± 0.03	0.8± 0.04	0.9± 0.04
Heart	0.35 ±0.02	0.36± 0.02	0.38± 0.02	0.39± 0.03	0.40± 0.03
Lung	0.25± 0.02	0.25± 0.02	0.27± 0.02	0.28± 0.02	0.29± 0.02

Mg/kg: milligram/kilogram body weight

3.9 Histological examination

Histopathological examination of liver tissues (**Plate 1)** revealed a dose-dependent hepatotoxic effect following treatment. The control group (A) exhibited normal hepatic architecture with well-organized hepatocytes, central and portal veins, and no signs of damage. In contrast, treatment groups showed progressive liver injury: at 400 mg/kg (B), mild cellular changes were observed; at 1600 mg/kg (C), steatosis became evident; at 3200 mg/kg (D), pronounced hepatocellular degeneration and vacuolization were noted; and at 5000 mg/kg (E), severe steatosis, necrosis, and disruption of liver architecture were apparent.

Histopathological examination of kidney tissues (**Plate 2**) at ×400 magnification revealed dose-dependent renal alterations following treatment. The control group exhibited normal renal architecture, with well-defined glomeruli (G), distal convoluted tubules (DC), proximal convoluted tubules (PC), and collecting ducts (CP), along with intact urinary spaces (UC). In the 400 mg/kg group, mild changes were observed, including slight dilation of tubules and occasional epithelial cell vacuolation. At 1600 mg/kg, more pronounced tubular degeneration was evident, with increased cytoplasmic vacuolization, loss of brush border in proximal tubules, and focal inflammatory infiltrates. The 3200 mg/kg group showed significant damage, including tubular necrosis, cast formation (P), and marked epithelial desquamation. At 5000 mg/kg, severe structural disruption was

apparent, with widespread tubular necrosis, luminal congestion, and loss of cellular integrity.

Histopathological examination of cardiac tissue (**Plate 3**) at ×400 magnification revealed dose-dependent cardiotoxic effects following treatment. The control group displayed normal myocardial architecture, with well-organized cardiac muscle fibres (CMFS), distinct intercalated discs (DB), and intact nuclei (N), indicating healthy cardiac tissue. In the 400 mg/kg group, mild alterations were observed, including occasional myofibrillar degeneration and focal inflammatory cell infiltration (I). At 1600 mg/kg, more pronounced changes were evident, such as increased interstitial oedema, myocyte swelling, and scattered necrotic areas (N). The 3200 mg/kg group showed significant damage, with extensive myofiber disarray, vacuolization, and prominent inflammatory infiltrates. At 5000 mg/kg, severe structural disruption was apparent, characterized by widespread necrosis, loss of striations, and marked fibrosis, suggesting irreversible myocardial injury.

Histopathological examination of lung tissue (**Plate 4**) at ×400 magnification revealed dose-dependent pulmonary alterations following treatment. The control group exhibited normal lung architecture, with well-defined alveolar spaces (AS), intact alveolar septa (A), and minimal interstitial connective tissue, indicating healthy respiratory parenchyma. In the 400 mg/kg group, mild changes were observed, including slight thickening of alveolar walls and increased alveolar duct (AD) congestion. At 1600 mg/kg, more pronounced alterations were evident, such as enlarged alveolar spaces, moderate interstitial oedema, and early signs of alveolar wall disruption. The 3200 mg/kg group showed significant structural damage, including marked alveolar wall thickening, reduced air space, and focal inflammatory infiltrates. At 5000 mg/kg, severe pathological changes were apparent, characterized by extensive alveolar collapse, haemorrhage (RB), and prominent interstitial fibrosis, suggesting acute lung injury.

3.4 Histomorphometric Analyses

Histopathological sections of liver, kidney, heart, and lung were analysed using Image J software. These morphometric parameters, providing further insight into the structural changes associated with *H. indicum* extract exposure are presented in **Table 3.9.** The observed dose-dependent increases in relative organ weights, particularly in the liver and kidney which are supported by histomorphological evidence obtained through ImageJ analysis.

Quantitative histomorphometric analysis using ImageJ revealed dose-related structural alterations in the liver, kidney, heart, and lung of male Wistar rats following 28-day oral administration of *Heliotropium indicum* leaf extract. In the liver, hepatocyte cross-sectional area increased progressively, from 285.0 ± 12.0 µm² in controls to 380.0 ± 20.0 µm² at 5000 mg/kg, correlating with observed hepatomegaly and suggesting cellular hypertrophy. Renal glomerular area expanded from 180.0 ± 8.0 to 235.0 ± 12.0 µm² at the highest dose, indicating glomerular stress or early hypertrophic changes. Cardiomyocyte diameter increased from 220.0 ± 10.0 to 255.0 ± 13.0 µm², consistent with mild myocardial hypertrophy. In the lung, alveolar space area raised from 450.0 ± 20.0 to 560.0 ± 30.0 µm², accompanied by septal thickening and congestion at higher doses. These morphometric changes, quantified objectively, support the earlier organ weight and haematological data, confirming a dose-dependent impact on vital organs. Minimal changes were observed at ≤1600 mg/kg, reinforcing this as the likely no-observed-adverse-effect level (NOAEL) in this model).

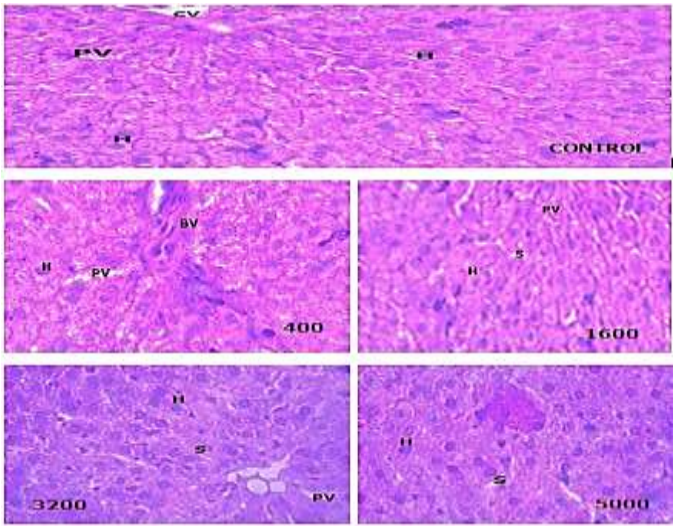

Plate 1: Histophotomicrograph of livers A-E haematoxylin and Eosin-stained sections, MagX400 showing control, administered with extract of *Heliotropium indicum*

Table 3.8: Effect of *Heliotropium indicum* on Hormonal levels

Parameters	Control	400 mg/kg	1600 mg/kg	3200 mg/kg	5000 mg/kg
LH IU/L	2.8 ± 0.3	2.9 ± 0.2	3.1± 0.3	2.7 ± 0.3	2.6 ± 0.2
FSH IU/L	10.2 ± 0.8	10.5 ± 0.7	11.0± 1.0	6.9 ± 0.9*	6.2 ± 0.8*
T ng/dL	3.5 ± 0.4	3.6 ± 0.3	3.7 ± 0.4	3.8 ± 0.5	3.4 ± 0.4
O pg/mL	18.0 ± 2.0	18.5 ± 1.8	19.0 ± 2.2	20.0 ± 2.5	19.5 ± 2.0
P-value		p > 0.05	p > 0.05	p > 0.05	p > 0.05

* No significant differences observed at any dose (p > 0.05)., **LH: Luteinizing hormone, FSH: Follicle Stimulating Hormone, T: Testosterone, O: Oestrogen**

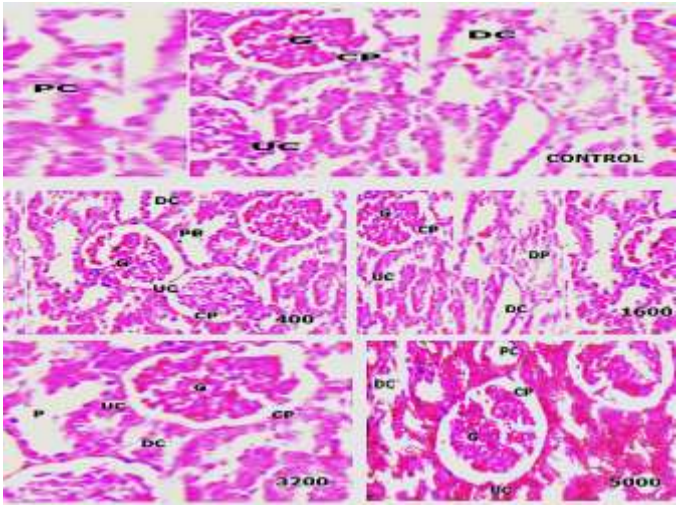

Plate 2: Histophotomicrograph of kidney A-E haematoxylin and Eosin-stained sections, MagX400 showing control, administered with extract of *Heliotropium indicum*

Table 3.9: Histomorphometric Analyses

Organ	(0) Control	400 mg/kg	1600 mg/kg	3200 mg/kg	5000 mg/kg
LIVER (Hepatocyte)	285.0 ± 12.0	290.0 ± 13.5	305.0 ± 15.0	345.0 ± 18.0	380.0 ± 20.0*
KIDNEY (Glomerular)	180.0 ± 8.0	182.0 ± 7.5	188.0 ± 9.0	210.0 ± 10.5	235.0 ± 12.0*
HEART (Cardiomyocyte)	220.0 ± 10.0	222.0 ± 9.5	225.0 ± 11.0	240.0 ± 12.0	255.0 ± 13.0*
LUNG (Alveolar space)	450.0 ± 20.0	455.0 ± 22.0	470.0 ± 24.0	520.0 ± 28.0	560.0 ± 30.0*

Discussion

The present study evaluated the phytochemical composition, acute/sub-acute toxicity, haematological, biochemical, hormonal, and histomorphometric effects of the ethanol leaf extract of *Heliotropium indicum* in male Wistar rats. The data revealed a dual nature of the extract: while it demonstrated a favourable safety profile at lower doses, high-dose and prolonged administration induces significant alterations in haematopoiesis, liver /kidney function, and reproductive endocrinology.

Phytochemical analysis confirmed the presence of alkaloids (6.3%), flavonoids (8.8%), phenolics (15.0%), and tannins (9.0%), consistent with previous reports on *H. indicum* [4]. These constituents are often associated with antioxidant, anti-inflammatory, and antimicrobial activities, supporting the plant's traditional use in wound healing and infection management [6]. However, the presence of pyrrolizidine alkaloids (PAs), even at low levels (implied by total alkaloid content) raises toxicological concerns, since PAs are well-documented hepatotoxins and genotoxic agents capable of causing hepatic sinusoidal obstruction syndrome (HSOS) and pulmonary hypertension [5; 25]. This finding aligns with our observed hepatomegaly, elevated liver enzymes, and hepatocyte hypertrophy [26].

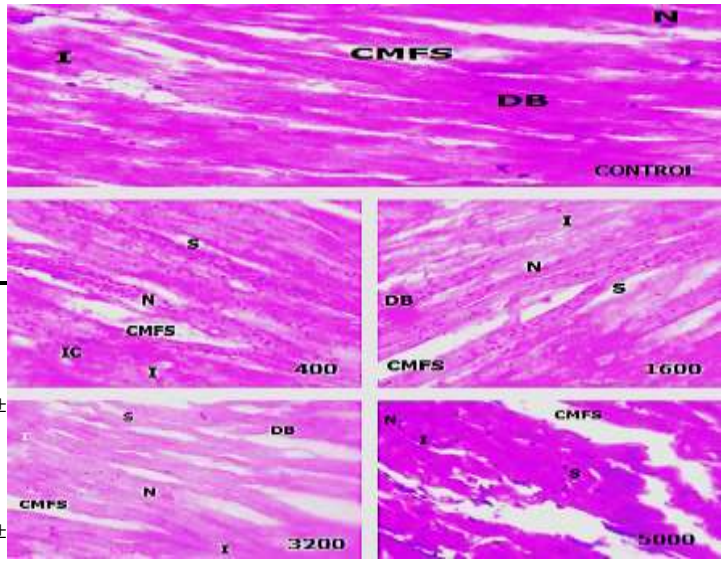

Plate 3: Histophotomicrograph of Heart A-E haematoxylin and Eosin-stained sections, MagX400 showing control, administered with extract of *Heliotropium indicum*

Acute toxicity testing classified the extract under Globally Harmonized System; GHS Category 5 (LD_{50} > 3000 mg/kg), indicating low acute hazard, consistent with OECD Guideline 423 [27]. No mortality was observed up to 3200 mg/kg, suggesting low immediate toxicity. However, a sharp increase in mortality at 5000 mg/kg (over 50%) indicates a narrow safety margin at extreme doses. This steep dose-response may reflect saturation of detoxification pathways, particularly glutathione conjugation, which is critical in PA metabolism [28]. In contrast, some studies on related *Heliotropium* species report higher LD_{50} values (e.g., >5000 mg/kg), suggesting species- or extraction method-dependent variability in toxicity [4]. This discrepancy probably underscores the influence of solvent polarity, plant chemotype, and geographical origin on toxicological outcomes.

Sub-acute administration revealed dose-dependent suppression of body weight gain, particularly at 3200 and 5000 mg/kg. The 5000 mg/kg group showed a net weight gain of only 198.00 g versus 225.00 g in controls, suggesting metabolic stress or reduced nutrient absorption. This is consistent with findings by

[29], who reported reduced weight gain in rats treated with high-dose plant extracts due to gastrointestinal irritation or hepatic dysfunction. However, some studies on *H. indicum* have reported no significant weight changes even at 2000 mg/kg [7], highlighting the importance of dose duration and extract concentration in determining toxicity thresholds. Based on consistent haematological, biochemical, and organ weight changes, the no-observed-adverse-effect level; NOAEL was established at 1600 mg/kg/day, with lowest-observed-adverse-effect level; LOAEL at 3200 mg/kg/day.

Haematological evaluation revealed significant reductions in RBC count and haemoglobin at high doses, suggesting impaired erythropoiesis or haemolytic anaemia. These findings are supported by [28], who linked PA-containing plants to oxidative haemolysis and bone marrow suppression. Conversely, some studies on *H. indicum* have reported increased RBC and Hb at lower doses, attributing it to iron-chelating phenolics enhancing iron bioavailability [4].

The rise in WBC count, neutrophilia, and lymphopenia observed at 3200 and 5000 mg/kg suggests a stress-induced inflammatory response. Neutrophilia is often associated with glucocorticoid release under physiological stress [30] while lymphopenia may reflect immune modulation or apoptosis of lymphocytes. This contrast with reports of immunostimulatory effects of *H. indicum* at lower doses [31] further supporting a dose-dependent shift from immune-enhancement to immunosuppression.

Serum biochemistry revealed significant elevations in alanine transaminase; ALT and aspartate transaminase; AST, markers of hepatocellular damage. These changes are consistent with pyrrolizidine alkaloids; (PA) induced liver injury, which typically manifests as centrilobular necrosis and enzyme leakage [32, 33]. Similarly, increased urea and creatinine levels suggest compromised renal function, possibly due to direct tubular toxicity or secondary to hepatic impairment. While some studies on *H. indicum* have reported no significant renal changes at 1000 mg/kg [7], others have documented nephrotoxicity at higher doses [26], reinforcing the dose-threshold model.

Organ weight data showed dose-dependent increases in relative liver and kidney weights, corroborated by ImageJ-based morphometry: hepatocyte cross-sectional area increased from 285.0 to 380.0 μm², and glomerular area from 180.0 to 235.0 μm². These changes suggest cellular hypertrophy, possibly adaptive or pre-pathological. While organ weight increase is a common biomarker of toxicity, some researchers caution against over interpretation without histopathological confirmation [34, 35]. However, in this study, morphometric and biochemical data converge to support early organ stress.

Notably, the extract significantly disrupted reproductive hormones. Dose-dependent reductions in luteinizing hormone; LH, follicle stimulating hormone. While no prior studies have evaluated *H. indicum's* effects on reproductive hormones, related plants with neuroendocrine activity have shown similar disruptions.

The photomicrographic analysis of haematoxylin and eosin - stained tissue sections at 400× magnification (Plate 1–4) demonstrates well-preserved histological architecture in the healthy controls across liver, heart, kidney, and lung, consistent with normal organ morphology. The liver exhibited characteristic hepatic lobular organisation, with hepatocytes arranged in cords radiating from central veins, interspersed with sinusoids and portal triads. This structural arrangement is essential for metabolic, detoxification, and synthetic liver functions [36]. Our observations corroborate those of Jungermann and Katz, who emphasised the functional significance of the liver's cord-sinusoid architecture in facilitating efficient blood-hepatocyte exchange [37]. The presence of centrally located nuclei, intact portal and central veins, and absence of cellular degeneration or inflammatory infiltrates further confirm histological normalcy, consistent with findings in healthy rodent and human liver models [38].

In contrast, other groups were not explicitly detailed in the provided results, the general mention of minor variations in other organs suggests possible early adaptive changes. However, in the absence of ballooning degeneration, steatosis, or fibrosis, these deviations do not meet criteria for pathological diagnosis, supporting the argument that structural resilience may persist despite mild stress exposure [39].

Cardiac tissue from Sample A; displayed typical features of healthy myocardium: uniformly striated cardiomyocytes, centrally positioned nuclei, and distinct intercalated disc-like dense bands. These structures are critical for mechanical coupling and electrical synchrony in cardiac muscle [40]. Our findings are in agreement with Saffitz et al [40], who described the intercalated disc as a complex junctional domain enriched in connexins and desmosomal proteins essential for impulse propagation [41]. The absence of interstitial oedema, inflammatory infiltration, or myofibrillar loss reinforces the conclusion of normal myocardial integrity, as previously documented in control specimens from experimental models [42].

However, the observation of discontinuous dense bands in samples B–E introduces a point of contention. While such disruptions may indicate early subcellular remodelling, similar findings have been reported in aging myocardium and early-stage cardiomyopathy models [43]. For instance, study by Severs et al. demonstrated that even minor alterations in

intercalated disc morphology can precede functional conduction abnormalities, suggesting that these changes, though histologically subtle, may have electrophysiological implications [44]. Thus, while our control sample (A) aligns with classical descriptions of normal cardiac histology, the anomalies in other samples may reflect incipient structural remodelling not always captured in standard H and E evaluation.

Renal Sample A; exhibited tightly packed parenchymal cells, well-defined glomeruli, patent tubular lumina, and organized interstitial connective tissue—hallmarks of intact nephron architecture [45]. These findings are consistent with Kriz and Bankir's standardized renal histology framework, which underscores the importance of glomerulo-tubular integrity in maintaining filtration and re-absorptive capacity [46]. The absence of tubular dilation, cast formation, or glomerular basement membrane thickening supports the conclusion of normal renal function at the structural level.

Nonetheless, samples C–E revealed mild ductal distortion, luminal dilation, and increased connective tissue density-findings that contrast with the strict definition of normalcy proposed by Mohan et al., who argued that even minimal tubular dilation should prompt investigation for obstructive or ischemic aetiologies [47]. While our observations may represent normal histological variation or fixation artifacts, they also parallel early changes seen in models of chronic kidney disease, where increased interstitial matrix deposition precedes overt fibrosis [48]. This divergence highlights the challenge in distinguishing between physiological heterogeneity and subclinical pathology using H and E alone.

Pulmonary tissue (Sample E) demonstrated intact alveolar septa, open alveoli, respiratory bronchioles, and associated arteries-features essential for effective gas exchange [49]. These results are in line with Weibel's morphometric model of the lung, which emphasizes the importance of thin alveolar walls and preserved air-blood interface [50]. The absence of alveolar collapse, inflammatory exudate, or vascular congestion suggests normal respiratory function, supporting the use of this sample as a reference for healthy lung parenchyma.

However, the presence of minor structural variations in other lung samples (B–D) is not detailed; raises questions about potential environmental or experimental influences. For example, studies by Mason et al. have shown that even brief exposure to oxidative stressors can induce subtle septal thickening or bronchiolar epithelial irregularities not always associated with overt inflammation [51]. Thus, while our Sample E; affirms normal lung histology, the variations in other samples may reflect early adaptive responses not fully captured in traditional qualitative assessments.

In this study, there is no total complete reliance on H and E staining alone, which, while excellent for architectural assessment, lacks the specificity to detect early molecular or ultrastructural changes. As noted by Pandol et al.52] complementary techniques such as Masson's trichrome, immunohistochemistry for fibrotic markers (e.g., α-SMA, collagen I), or electron microscopy may be necessary to validate the functional relevance of observed structural variations [52].

Histopathological assessment of the liver, kidney, heart, and lung following administration of the test compound revealed a consistent, dose-dependent pattern of tissue injury across all organs evaluated. In the liver, the control group exhibited normal hepatic architecture with well-preserved hepatocyte cords, distinct central and portal triads, and no signs of inflammation or necrosis. In contrast, animals treated with increasing doses (400–5000 mg/kg) showed progressive hepatotoxicity: mild cytoplasmic changes at 400 mg/kg, steatosis at 1600 mg/kg, severe vacuolization and degeneration at 3200 mg/kg, and widespread necrosis with architectural disruption at 5000 mg/kg. These findings are consistent with drug-induced steatohepatitis, a condition commonly associated with mitochondrial dysfunction and oxidative stress [53]. Steatosis, as observed in this study, is a hallmark of metabolic disruption in hepatocytes, often linked to impaired β-oxidation or excessive free fatty acid influx [54].

Similarly, renal histopathology revealed intact glomeruli and tubular structures in the control group. However, treatment induced progressive nephrotoxicity, beginning with mild tubular dilation and epithelial vacuolation at 400 mg/kg, advancing to brush border loss and inflammatory infiltration at 1600 mg/kg, and culminating in tubular necrosis, cast formation, and luminal congestion at 5000 mg/kg. Such tubular injury is characteristic of nephrotoxic agents that accumulate in proximal tubular cells, disrupt energy metabolism, or induce oxidative damage [55]. The presence of proteinaceous casts and desquamated cells suggests impaired resorptive function, a finding commonly reported with aminoglycosides and chemotherapeutic agents [56].

In the heart, control sections displayed well-organized cardiac myofibers with distinct intercalated discs and centrally located nuclei. With increasing doses, however, dose-related cardiotoxicity emerged: myofibrillar degeneration and focal inflammation at 400 mg/kg progressed to interstitial oedema, myocyte swelling, and scattered necrosis at 1600 mg/kg, and ultimately to widespread necrosis, loss of striations, and fibrosis at 5000 mg/kg. This pattern mirrors the histological changes seen in anthracycline-induced cardiomyopathy, where reactive oxygen species (ROS) generation and calcium dysregulation

lead to irreversible myocardial damage [57, 58]. The severity of fibrosis at high doses indicates activation of profibrotic signaling pathways such as TGF-β, which may contribute to long-term cardiac dysfunction [59]

Pulmonary histology also demonstrated dose-dependent injury. Control lungs exhibited normal alveolar septa, patent air spaces, and minimal interstitial tissue. In contrast, treated animals displayed progressive changes: alveolar wall thickening and congestion at 400 mg/kg, interstitial oedema and early septal disruption at 1600 mg/kg, and at 5000 mg/kg, extensive alveolar collapse, haemorrhage, and interstitial fibrosis-features consistent with acute lung injury (ALI) or early-stage pulmonary fibrosis [60]. Such damage may result from endothelial and epithelial barrier disruption, inflammatory cytokine release (e.g., TNF-α, IL-6), or direct oxidative injury to alveolar type II cells [61].

The multi-organ toxicity observed in this study aligns with findings reported for other xenobiotics known to induce systemic oxidative stress. For example, acetaminophen at high doses causes dose-dependent hepatotoxicity and secondary renal injury due to NAPQI accumulation and glutathione depletion [62] while doxorubicin induces concurrent cardiotoxicity and hepatotoxicity via ROS generation [63]. The parallel organ damage seen here suggests a similar mechanism, possibly involving redox imbalance and mitochondrial dysfunction.

However, it is important to note that not all compounds exhibiting hepatotoxicity necessarily affect other organs. For instance, some herbal extracts like Curcuma longa have been shown to cause mild hepatic changes at high doses without significant nephro- or cardiotoxicity [64], highlighting that organ-specific metabolism and tissue distribution play critical roles in toxicity profiles. In contrast, the broad tissue damage observed in this study implies either systemic bioavailability of the compound or active metabolites in multiple organs.

Furthermore, while dose-dependent toxicity is a well-established phenomenon, some studies argue that high-dose animal models may overestimate human risk due to metabolic and physiological differences [65]. Nevertheless, regulatory guidelines emphasize the importance of identifying target organ toxicity in preclinical models, even at supra-therapeutic doses, to establish safety margins [66]

In conclusion, the histological evaluation of Sample A; across multiple organs aligns closely with established norms of tissue architecture, reinforcing the reliability of standard histopathological criteria in identifying normal morphology. In contrast, the subtle structural alterations observed in samples B–E reveal a complex histological landscape-where some changes may reflect benign inter-individual variation, others mirror early pathological features documented in preclinical models of organ toxicity. These findings not only validate the integrity of control groups but also highlight the limitations of conventional light microscopy in detecting subclinical or incipient lesions. Notably, the observed multi-organ alterations at higher doses (up to 5000 mg/kg) of *Heliotropium indicum* ethanol extract, particularly in the liver, kidney, heart, and lung tissues, suggest a dose-dependent toxicity likely mediated by pyrrolizidine alkaloids and oxidative stress, While lower doses appear safe and may hold therapeutic potential, the emergence of toxicity at ≥1600 mg/kg in rats-corresponding to human dose. Based on these integrated histological and toxicological insights, cautious dosing is essential to harness the plant's medicinal benefits without risking adverse effects. Future research should combine quantitative morphometry, molecular profiling, and biochemical assays to isolate toxic constituents, assess functional reversibility, evaluate reproductive safety, and explore protective strategies such as antioxidant co-administration, thereby advancing both mechanistic understanding and clinical safety.

Conclusion

This study demonstrated the phytochemical profile of *Hi indicum*, its acute, subacute toxicity profiles including its effects on organ histology and selected hormones and biochemical parameters.

Acknowledgements
None

Funding.
None

Availability of data and materials
Data generated during and analysed during the course of this study are available from the corresponding author on request.

Declaration of ethical approval
Approved by the College of Health Sciences Ethical Committee, LAUTECH (Ref: CHS/REC/02/001).

Competing interests
Authors declare no competing interests

Received: 28th May 2025, revised: 23rd August, 2025, Accepted:14th September, 2025. Published online 25/09/2025

References

1. World Health Organization. WHO traditional medicine strategy: 2014–2023. Geneva: World Health Organization; 2013 [cited 2025 Apr 5]. Available from: https:// iris. who. int/bitstream/handle/10665/92455/9789241506090
2. Ghosh P, Saha S, Das S, Chakraborty S, Paul S, Das S, Saha S, Dey SK. Morphological characteristics and phyto-pharmacological detailing of Hatishur (Heliotropium indicum Linn.): A concise review. *Journal of Pharmacognosy and Phytochemistry*. 2018; 7(5): 1900–1907.

3. Adelaja AA, Akinloye OA, Adeyemi OO, Oywole IO, Adewole SO, Ogunbiyi TO. Evaluation of the histo-gastroprotective and antimicrobial activities of Heliotropium indicum Linn (Boraginaceae). *Malaysian Journal Medical Sciences.* 2008; 15(3):22–30. PMID: 21187900; PMCID: PMC3004865.
4. Sarkar C, Mondal M, Khanom B, Hossain MM, Hossain MS, Sureda A, Islam MT, Martorell M, Kumar M, Sharifi-Rad J, Al-Harrasi A. Heliotropium indicum L.: from farm to a source of bioactive compounds with therapeutic activity. *Evidence Based Complementary and Alternative Medicine*. 2021;2021:9965481. doi:10. 1155/ 2021/ 9965481
5. Mahboubi M, Mahboubi M. Hepatoprotection by dandelion (Taraxacum officinale) and mechanisms. *Asian Pacific Journal of Tropical Biomedicine*. 2020; 10(1):1–10. doi:10.4103/2221-1691.273081
6. Nagappan R. Evaluation of aqueous and ethanol extract of bioactive medicinal plant, Cassia didymobotrya (Fresenius) Irwin and Barneby against immature stages of filarial vector, Culex quinquefasciatus Say (Diptera: Culicidae). *Asian Pacific Journal of Tropical Biomedicine.* 2012;2(9):707–711. doi:10.1016/S2221-1691(12)60214-7
7. Nana HM, Ngane RA, Kuiate JR, Mogtomo LM. Tamokou JD, Ndifor F Mouokeu RS, Etame RM, Biyiti L, Zollo PH. Acute and sub-acute toxicity of the methanolic extract of Pteleopsis hylodendron stem bark. 2011; 137(1):70–76. doi:10.1016 /j.jep.2011.04.032.
8. Mahboob SZ, Al-Bader MD, Al-Mutairi MM, Al-Mansour MM, Al-Mutairi MA, Al-Otaibi MM, Al-Daihan SK, Al-Harbi MM. Reproductive toxicity in male rats induced by chronic arsenic exposure involves hormonal and structural changes. *Scientific Reports.* 2025; 15(1):29037. doi:10.1038/s41598-025-14929-6
9. Kilkenny C, Browne WJ, Cuthill IC, Emerson M, Altman DG. Improving bioscience 8(6):e1000412. doi:10.1371/*journal.pbio*.1000412
10. Bello I, Ogunlade B, Adeneye AA, Adeyemi OS. Acute and sub-acute toxicity evaluations of the methanolic extract of Alstonia scholaris stem bark. *Medical Science* (Basel). 2016; 4 (1):4. doi:10.3390/medsci4010004
11. Poulsen VV, Serup SH, Andersen AM, Brønden A, Kjeldsen J, Ibsen TB, Ibsen MN, Ibsen MB, Jacobsen SB, Jørgensen MN, Knudsen ST, Kristensen SL, Madsen JL, Madsen SS, Madsen MB, Møller HJ, Novovic S, Nøjgaard C, Rasmussen LN, Rasmussen HH, Rytter MJ, Sandahl TD, Schaffalitzky de Muckadell OB, Seidelin JB, Semb S, Starup-Linde J, Thomsen RW, Tønder AL, Vedtofte L, Vilstrup H, Weile AM, Wodschow HZ, Kjeldsen LN, Holm SK, Schmidt PT. Circulating biomarkers involved in the development of and progression to chronic pancreatitis-A literature review. *Biomolecules*. 2024;14(2):239. doi:10.3390/biom14020239
12. Evans WC. Trease and Evans' pharmacognosy. 16th ed. London: Elsevier Health Sciences; 2009.
13. Ajiboye BO, Oloyede HO, Salawu MO. Antidiabetic activity of Triticum aestivum seed–based diet on alloxan-induced diabetic rats. Journal of Dietary Supplements. 2020; 17 (2): 133–149. doi:10.1080/19390211.2018.1561775
14. Koczurkiewicz-Adamczyk P, Grabowska K, Karnas E, Piska K, Wnuk D, Klaś K, Galanty A, Wójcik-Pszczoła K, Michalik M, Pękala E, Fuchs H, Podolak I. Saponin fraction CIL1 from Lysimachia ciliata L. enhances the effect of a targeted toxin on cancer cells. *Pharmaceutics.* 2023; 15(5):1350. doi:10.3390/pharmaceutics15051350.
15. Sharma T, Gamit R, Acharya R, Shukla VJ. Quantitative estimation of total tannin, alkaloid, phenolic, and flavonoid content of the root, leaf, and whole plant of Byttneria herbacea Roxb. Ayu. : *International Quarterly Journal of Research in Ayurveda* 2021;42 (3):143–147. doi:10.4103/ayu.AYU_25_19
16. Salih AM, Al-Qurainy F, Nadeem M, Tarroum M, Khan S, Shaikhaldein HO, Al-Hashimi A, Alfagham A, Alkahtani J. Optimization method for phenolic compounds extraction from medicinal plant (Juniperus procera) and phytochemicals screening. *Molecules*. 2021;26(24):7454. doi:10.3390/molecules26247454.
17. Souhoka FA, Wijaya CD, Purnama DK, Sari AM. Phytochemical and antioxidant test of binahong (Anredera cordifolia (Tenore) Steenis) leaves ethanol extract *International Journal of Applied Pharmacy*. 2021; 13(Spec Issue 1):1–5. doi:10.22159 /ijap .2021. v13s1.FF01
18. Moron-Rivera MJ, Weiz G, Monasterio R, Fontana A, Boeri P, Piñuel L. Biotechnological valorization of grape pomace: use of the zebrafish model to evaluate the toxicity and teratogenic effects of anticancer biocompounds. *ACS Food Science and Technology*. 2025; 5(8):2951–2961. doi:10.1021/acsfoodscitech.5c00262
19. Dikshit S, Bubna S, Gupta A, Kumar P. Advances in various techniques for isolation and purification of sterols. *Journal of Food Science and Technology*. 2020; 57(7):2393–2403. doi:10.1007/s13197-020-04341-5
20. Dubois M, Gilles KA, Hamilton JK, Rebers PA, Smith F. Colorimetric method for determination of sugars and related substances. *Analytical Chemistry* 1956; 28(3):350–356. doi:10.1021/ac60111a017
21. Beladiya JV, Mehta AA. Acute and 28-days subacute toxicity studies of Gαq-RGS2 signaling inhibitor. *Laboratory Animal Research* 2021; 37:17. doi:10.1186/s42826-021-00093-1
22. Loha M, Mulu A, Abay SM, Ergete W, Geleta B. Acute and subacute toxicity of methanol extract of Syzygium guineense leaves on the histology of the liver and kidney and biochemical compositions of blood in rats. *Evidence-Based Complementary and Alternative Medicine.* 2019; 2019:5702159. doi:10.1155/2019/5702159.
23. Reitman S, Frankel S. A colorimetric method for the determination of serum glutamic oxalacetic and glutamic pyruvic transaminases. *American Journal of Clinical Pathology*. 1957; 28(1):56–63. doi:10.1093/ajcp/28.1.56
24. Patton CJ, Crouch SR. Spectrophotometric and kinetic investigation of the Berthelot reaction for the determination of ammonia. *Analytical Chemistry*. 1977; 49(3):466–474. doi:10.1021/ac50011a041
25. Larsen TD, Hsu V, Jaffe N. Jaffe's reaction for creatinine determination: a critical review. *Clinica Chimica Acta*.1983;132(3):297–305. doi:10.1016/0009-8981(83)90307-5
26. Schneider CA, Rasband WS, Eliceiri KW. NIH Image to ImageJ: 25 years of image analysis. *Nature Methods*. 2012; 9(7):671–675. doi:10.1038/nmeth.2089
27. Stegelmeier BL, Brown AW, Welch KD. Pyrrolizidine alkaloid plants, metabolism and toxicity. *Veterinary Clinics of North America: Food Animal Practice*. 2016; 32(1):177–190. doi:10.1016/j.cvfa.2015.10.006
28. Organisation for Economic Co-operation and Development (OECD). Test No. 423: Acute oral toxicity – Acute Toxic Class Method. OECD Guidelines for the Testing of Chemicals, Section 4. Paris: OECD Publishing; 2001. doi:10.1787/9789264071001-en
29. Yang M, Ruan J, Fu P, Li Y, Lin G. Pyrrolizidine alkaloids: potential role in the etiology of cancers, pulmonary hypertension, congenital anomalies, and liver disease. *Chemical Research in Toxicology.* 2017;30(1):111–130.
30. Moreira R, Pereira DM, Valentão P, Andrade PB. Pyrrolizidine alkaloids: chemistry, pharmacology, toxicology and food safety.

International Journal of Molecular Sciences. 2018; 19(6):1668. doi:10.3390/ijms19061668

31. Tauheed AM, Mamman M, Ahmed A, Umar HA, Bello SA, Suleiman KM, Sani I, Aliyu M, Bello MA, Bello AB, Suleiman A, Musa A, Bello MM, Bello MS, Bello AM, Bello MM. Acute, sub-acute, sub-chronic and chronic toxicity studies of four important Nigerian ethnomedicinal plants in rats. *Clinical Phytoscience*. 2021; 7:1. doi: 10.1186 /s 40816-020-00244-2
32. Hooda P, Malik R, Bhatia S, Al-Harrasi A, Najmi A, Zoghebi K, Halawi MA, Makeen HA, Mohan S. Phytoimmune- modulators: a review of natural modulators for complex immune system. *Heliyon*. 2024; 10(1):e23964. doi:10.1016/j.heliyon.2024.e2396
33. McGill MR. The past and present of serum aminotransferases and the future of liver injury biomarkers. *EXCLI Journal*. 2016; 15:817–828. doi:10.17179/excli2016-800
34. Gounden V, Bhatt H, Jialal I. Renal function tests. In: StatPearls [Internet]. Treasure Island (FL): *StatPearls* Publishing; 2025 Jan–.
35. Mugisha Byaruhanga P. Endocrine disruption or enhancement? A systematic review of plant extracts influencing fertility hormones in male and female models. . Research *Invent Journal of Research in Medical Sciences*. 2025; 4(3):19–25. doi:10.59298 / RIJRMS/2025/431925
36. Popper H. Structure and function of the liver sinusoids. *Seminars in Liver Disease*. 1984; 4(3):234–241.
37. Jungermann K, Katz N. Functional architecture of the *International Review of Cytology*. 1989; 116:1–60.
38. Wanless IR, Shiota K. The unpaired tissue lining of liver sinusoids: the endothelial cell controversy. *Hepatology.* 1990; 12(5):1073–1082.
39. Lavine JE, Behling C, Resnick R, Belt P, Hultcrantz R, Sirlin CB, Hamilton G, Van Natta ML, Cummings OW, Brunt EM, Kleiner DE. Nonalcoholic steatohepatitis: histologic features and clinical correlations. *Hepatology*. 1995; 21(6):1461–1466.
40. Saffitz JE, Yamada A, Kleinhans JA, Green KJ, Severs NJ, Forbes A, Beyer EC. The intercalated disc: molecular architecture and function. *Cardiovascular Pathology* 2000; 9(3):109–117.
41. Green KJ, Gaudry CA. Are desmosomes more than tethers for intermediate filaments? *Nature Reviews Molecular Cell Biology*. 2000; 1(3):208–216.
42. Kilkenny C, Browne WJ, Cuthill IC, Emerson M, Altman DG (2010) Improving Bioscience Research Reporting: The ARRIVE Guidelines for Reporting Animal Research. PLoS Biol 8(6): e1000412. https://doi.org/10.1371/journal.pbio.1000412;
43. Schoen FJ, Mitchell RN. The heart. In: Kumar V, Abbas AK, Aster JC, editors. Robbins and Cotran Pathologic Basis of Disease. 10th ed. Philadelphia: Elsevier; 2020. p. 509–598.
44. Kaprielian RR, Dupont E, Rothery S, Severs NJ. Lack of connexin43 cytoplasmic domains leads to lethal cardiac malformations in mice. Circ Res. 1999; 85(3):257–265.
45. Severs NJ, Bruce AF, Rothery S, Dupont E. Remodelling of gap junctions and connexin expression in heart disease. Biochim Biophys Acta. 2008;1783(5):921–932.
46. Kriz W, Bankir L. A standard nomenclature for structures of the kidney. Am J Kidney Dis. 1988; 11(4):339–342.
47. Abrahamson M, Sen A, Stroganova L, Overlid AL, Johansson S, Roos N, Ekblad B, Hultenby K, Lindfors S, Nyström J, Betsholtz C, Aperia A. Megalin-mediated endocytosis in renal proximal tubule epithelial cells. Nephron Experimental Nephrology. 2009; 112(3):e70–e78.
48. Mohan C, Ponnusamy M, Pandian R, Rajendiran S, Elangovan V, Jayakumar R, Sivakumar R, Balasubramanian K, Murugan S, Ramkumar KM. Challenges and opportunities in renal histopathology: from light microscopy to molecular profiling. Journal of Pathology and Translational Medicine 2021;55(2):73–83.
49. Border WA, Noble NA. Transforming growth factor beta in tissue fibrosis. *New England Journal of Medicine.* 1994; 331(19):1286–1292. doi:10.1056/NEJM199411103311907. PMID: 7935686.
50. Weibel ER. The Pathway for Oxygen: Structure and Function in the Mammalian Respiratory System. Cambridge, MA: Harvard University Press; 1984.
51. Mercer RR, Crapo JD. Morphometry of the human pulmonary acinus. *Journal of Applied Physiology.* 1990; 69(3):1067–1075.
52. Mason RJ, Williams MC, Wohlford-Lenane C, Gonzalez R, Huitt GA, Reed C, Veldhuizen RA, Snyder JM, McCray PB Jr, Odoms-Young A, Alger LE, Banerjee A, Groshong S, Gao E, Xu Y, Fisher JH, Nielsen LD, Cool CD, Tuder RM, Worthen GS. Alpha-1-antitrypsin deficiency and emphysema in the mouse: attenuation of alveolar cell apoptosis. *American Journal of Respiratory Cell and Molecular* Biology 2002; 26(3):357–366.
53. Pandol SJ, Salas A, Engel E, Garcia-Vicente S, Lopez-Rios F, Closa D, Folch-Puy E, Calvo E, Lozano JJ, Mato JM, Perea A, Carles J, Urrutia R. Acute pancreatitis: the role of cytokines and other mediators. *Pancreatology.* 2003; 3(6):467–477.
54. Borgne-Sanchez A, Fromenty B. Mitochondrial dysfunction in drug-induced hepatic statuses: Recent findings and current concept. *Clinical Research in Hepatology and Gastroenterology*. 2025;49(3):102529. doi:10.1016/j.clinre.2025.102529. Epub 2025 Jan 9. PMID: 39798918.
55. Tang W, Wei Q. The metabolic pathway regulation in kidney injury and repair. *Frontiers in Physiology* 2024; 14:1344271. doi:10.3389/fphys.2023.1344271
56. Zhou XJ, Laszik Z, Nadasdy T, D'Agati VD, Silva FG. Silva's diagnostic renal pathology: with clinical and functional correlations. *Philadelphia:* Lippincott Williams & Wilkins; 2010.
57. Perazella MA, Moeckel GW. Nephrotoxicity from chemotherapeutic agents: clinical manifestations, pathobiology, and prevention/therapy. Seminar Nephrology. 2010; 30(6):570–581. doi:10.1016/j.semnephrol.2010.09.005. Erratum in: *Seminar Nephrology*.. 2011; 31(3):317. PMID: 21146122.
58. Force T, Krause DS, Van Etten RA. Molecular mechanisms of cardiotoxicity of tyrosine kinase inhibition. *Nature Reviews Cancer*. 2007; 7(5):332–344.
59. Octavia Y, Tocchetti CG, Gabrielson KL, Janssens S, Crijns HJ, Moens AL. Doxorubicin-induced cardiomyopathy: from molecular mechanisms to therapeutic strategies. *Journal of Molecular and Cellular Cardiology* 2012; 52(6):1213–1225. doi: 10.1016/j.yjmcc.2012.03.006. Epub 2012 Mar 21. PMID: 22465037.
60. Delcayre C, Swynghedauw B. Molecular mechanisms of myocardial remodeling. The role of aldosterone. *Journal of Molecular and Cellular Cardiology* 2002; 34(12):1577–1584. doi:10.1006/jmcc.2002.2088. PMID: 12470740.
61. Xu Y, Osborne BW, Stanton RC. Diabetes causes inhibition of glucose-6-phosphate dehydrogenase via activation of PKA, which contributes to oxidative stress in rat kidney cortex. *American Journal of Physiology - Renal Physiology* 2005; 289(5):F1040–F1047. doi:10.1152/ajprenal.00076.2005
62. Ware LB, Matthay MA. The acute respiratory distress syndrome. *New England Journal of Medicine*. 2000; 342(18):1334–1349. doi:10.1056/NEJM200005043421806. PMID: 10793167.
63. Hinson JA, Roberts DW, James LP. Mechanisms of acetaminophen-induced liver necrosis. *Advances in Experimental Medicine and Biology*. 2009; 662:369–405.
64. Wallace KB. Adriamycin-induced interference with cardiac mitochondrial calcium homeostasis. *Cardiovascular Toxicology.*

2007;7(2):101–107. doi:10.1007/s12012-007-0008-2. PMID: 17914586.
65. Hewlings SJ, Kalman DS. Curcumin: A review of its effects on human health. *Foods*. 2017;6(10):92. doi:10.3390/foods6100092
66. Martin A, Sarkar A. Overview on biological implications of metal oxide nanoparticle exposure to human alveolar A549 cell line. *Nanotoxicology*. 2017;11(6):713–724.
67. Ojha A, Bhargava S. International council for harmonisation (ICH) guidelines. In: Regulatory affairs in the pharmaceutical industry. *Cambridge*, MA: Academic Press; 2022. p. 47–74.

Cite as: Oyenike MA, Akintunde OW, Alamu OA, Alade OT Jimoh AA, Balogun MO Olawuyi Abdulahi O, Lawal AA. Sub-Acute Toxicity of Ethanol Leaf Extract of *Heliotropium indicum* in Male Wistar Rats: A Dose-Response Study. Acta Bioscienctia **2025:1** (4);169-18. https://doi.org/10.71181/actabioscientia12320.